Synthesis and Characterization of Microcapsules for Self-Healing Materials

Emma Shansky

Research Advisor: Dr. Jeffrey M. Zaleski

C500 Final Report
April 21st, 2006

Department of Chemistry
Indiana University
Bloomington, IN 47405

Abstract

This paper describes the progress made toward synthesis and characterization of microencapsulated monomers dicyclopentadiene and cyclooctadiene, spectroscopic evaluation of the microcapsules in an original self-healing material, and spectroscopic distinctions between monomer and polymer. Methods of characterization described include infrared, Raman, and fluorescence spectroscopy as well as SEM images. Brief discussions of self-healing materials, ring-opening metathesis polymerization (ROMP), and the mechanism and controlling parameters of microencapsulation are included.

Introduction: A "Self-Healing" System

Inspired by biological systems, the "self-healing" concept has recently been applied to synthetic materials as a way to repair micro-scale damage. Self-healing materials, though still in the early stages of design, may have applications in systems where detection and repair of damage is limited, if not impossible. For example, undetected microcracks in space- and aircrafts can multiply over time, compromising the strength of the material and often resulting in irreparable damage.[1]

The Original Design

A material that can "sense" its own degradation and repair itself automatically has already been designed and has been shown to have enhanced mechanical properties. The original design includes the presence of microencapsulated monomers and catalyst particles in an epoxy resin. This scheme employs dicyclopentadiene (DCPD) as the monomer and a

microcapsule outer shell composed of poly(urea-formaldehyde) and inner shell of ethylene maleic anhydride copolymer (EMA) (Figure 1).

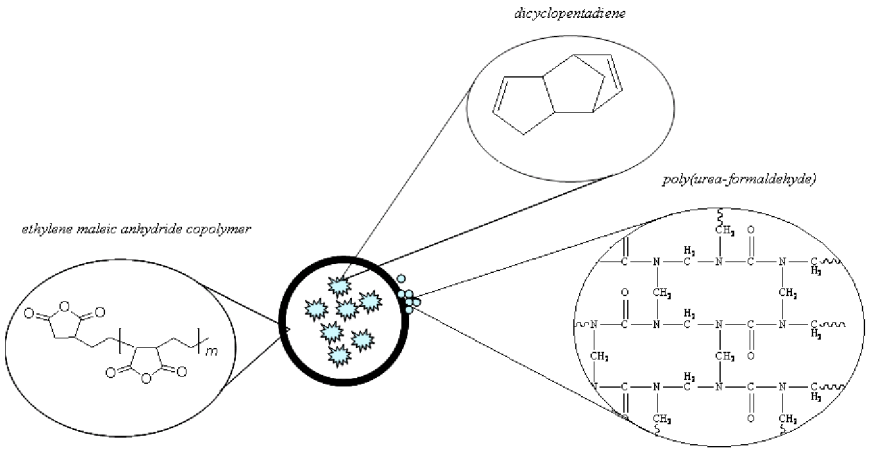

Figure 1. Composition of microcapsules.

Microcapsules containing the organic liquid-phase monomer are dispersed among a polymeric matrix. As a microcrack grows within the matrix, it punctures the microcapsule shell, causing the monomer to flow into the crack. Upon contact with a catalyst particle, the monomer undergoes a polymerization reaction. The cross-linked polymer product acts as a solid-phase "glue" to reduce further crack propagation, which increases the lifetime of the material.[2a,b,c] The general mechanism is outlined in Figure 2.

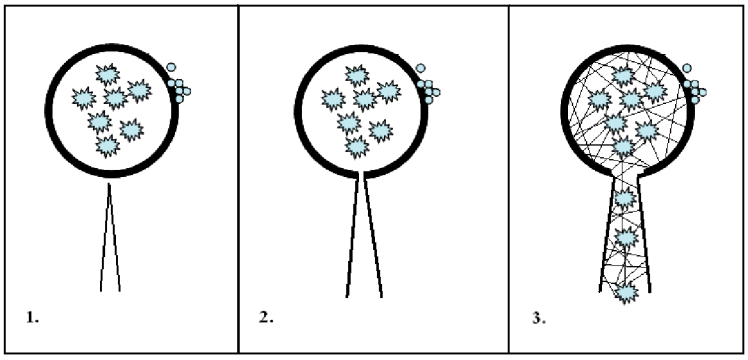

Figure2. Self-healing mechanism; 1) propagation of microcrack; 2) puncture of the microcapsule shell; 3) healing agent released in the crack.

The success of this system, however, may be overshadowed by several limitations:

- **DCPD has a melting point at 37°C.** The microencapsulated monomer must be in the liquid phase in order to flow through the damage site. The original design is ineffective at low temperatures because DCPD is very likely in the solid phase. Diffusion of solid phase DCPD into the crack is slow or unlikely to occur at all.
- **Epoxy resins have strong adhesive properties.** EPON 828, the epoxy resin used in the original design, is strongly adhesive to a wide variety of substrates. This property secures microcapsules within the matrix, preventing slippage and increasing the effects of cracks and other disturbances on the microcapsule. For polymers with weak or no adhesive properties, the microcapsules may be allowed more mobility within the matrix and might lose sensitivity to disturbances. The self-healing capabilities of microcapsules need to be tested in a non-adhesive polymer matrix.
- **The microcapsules are injected into a damage-prone site.** By intentionally loading the microcapsules between two layers of epoxy followed by the instigation of a "pre-crack," the system is predisposed to cracking and sliding in this rift. The highly-controlled environment in which the self-healing capabilities of the system are studied is not realistic for non-academic applications.

The Modified Design

In order to address these limitations, appropriate modifications have been made to the self-healing system. We are exploring the use of different monomers that can undergo Grubbs'

catalyzed ring-opening metathesis polymerization (ROMP) at room temperature. These monomers necessarily have melting points below 23°C, preferably even lower in order to accommodate use in space applications. The monomers currently being explored as part of our new self-healing design include 1,5-cyclooctadiene (COD), 1,3,5,7-cyclooctatetraene, and cyclooctene, with melting points -70°C, -27°C, and -16°C, respectively. Successful microencapsulation of 1,5-cyclooctadiene has been achieved and incorporated into our modified self-healing system. Spectral evidence has been obtained for the formation of DCPD as well as COD microcapsules (Figures 5-).

The epoxy matrix in which the microcapsules are embedded is being replaced by low-cost, transparent polymers; including polystyrene (PS), polymethylmethacrylate (PMMA), and polystyrene-polyisoprene-polystyrene block copolymer (SIS). These polymers have relatively good mechanical and electrical properties and good protection against gamma radiation.[3] The weak adhesive properties of these polymers allow analysis of the self-healing capabilities in environments more realistic for aerospace applications.

The final modification from the original self-healing design is the sample preparation. All samples consist of a homogeneous polymer solution embedded with microcapsules and catalyst. Sample preparation is simple, making our methods more conducive to industrial production. And, cracks are not initiated manually, so the study more closely resembles realistic conditions. Preliminary results of material strength testing reveal enhanced mechanical properties of our modified self-healing system, although these results will not be discussed in this paper.

Mechanism of Microcapsule Formation

Microencapsulated organic molecules are most commonly found in pharmaceutical drug design as time-released agents. Microencapsulated corrosion-prevention agents are often incorporated in paint as well. And, microencapsulated fragrances are contained in perfume, lotion, and "scratch-and-sniff" stickers. The widespread applications for microcapsules have made their formation a well-understood and easily-controlled process.

Our procedure for generating microcapsules is outlined by Brown, et al.[4] The mechanism by which microcapsules form begins with the presence of the EMA copolymer in water. Under continuous agitation, the organic monomer is introduced and drawn to the nonpolar side of EMA. EMA wraps itself around the monomer in a micelle-like formation, shielding the organic phase from the aqueous phase. Meanwhile, the poly(urea-formaldehyde) condensation reaction has begun in the aqueous phase. The polymer begins growing at the emulsion interface as its solubility decreases, resulting in a highly cross-linked shell wall.[5a,b] This process is known as *in situ* microencapsulation (Figure 3).

Much of the urea-formaldehyde prepolymer formed in the aqueous phase begins attaching itself to the outer shell. This causes the rough topology of the microcapsules. Carefully outlined by Brown, et al. are also the parameters that control microcapsule shell thickness, surface morphology, and diameter.[4]

1 *EMA copolymer in water*

2 *poly(urea-formaldehyde) condensation*

3 *EMA micelle formation around monomer and formation of shell wall*

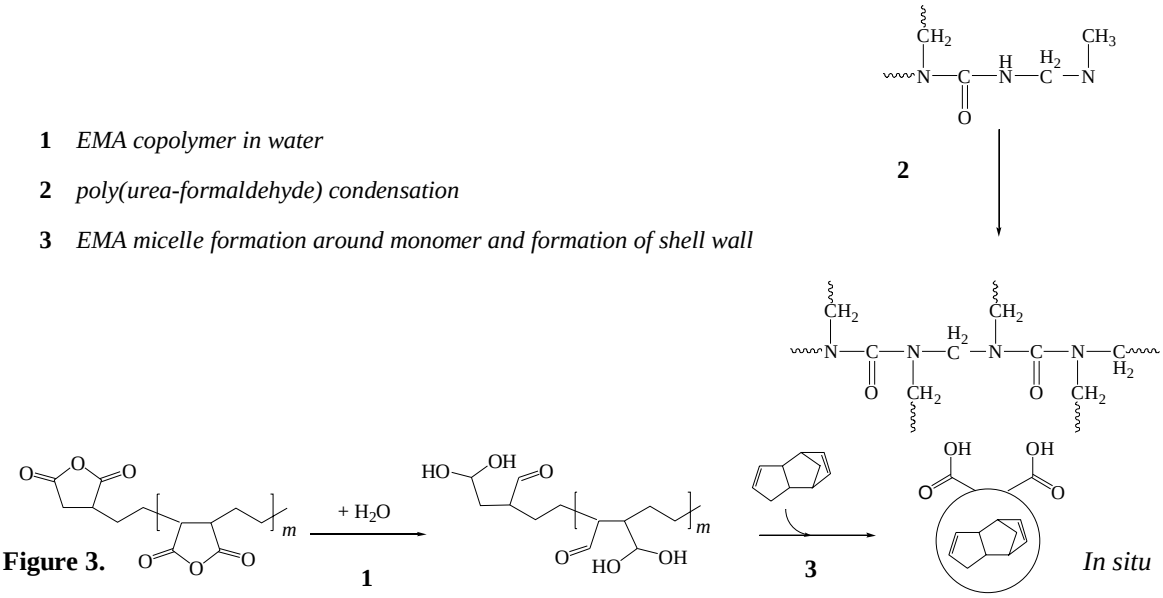

Figure 3. microencapsulation of dicyclopentadiene.

Controlling the Characteristics of Microcapsules

A brief discussion of the parameters that control the size, morphology, and shell wall thickness is useful in order to understand the conditions under which the microcapsules were prepared. While still under investigation, some of the desired qualities and the parameters necessary to achieve those qualities are highlighted.

Size

The optimum microcapsule diameter is yet to be determined. However, the controlling parameter is the agitation rate. Producing micron-scale spheres (10-1000 µm) requires 200-2000 rpm agitation.[4] At 550 rpm, the average diameter is about 200 µm at 79-92% yield, according to Brown, et. al. Our microcapsules were thus prepared using 450-550 rpm agitation rate.

Morphology

In order to optimize any adhesive properties of the microcapsules to the polymeric matrix, a rough surface morphology is desired. The condensation reaction to produce poly(urea-formaldehyde) requires either basic or acidic conditions. When the reaction begins at pH ~3.5, a subsequent decrease to pH ~2.5 occurs naturally. This accelerates the polymerization rate, which increases the viscosity of the reaction mixture. The organic-aqueous interfacial tension is hence increased and urea-formaldehyde prepolymer clusters aggregate at this interface.[6] The formation of urea-formaldehyde aggregates can also be increased by decreasing the agitation rate and/or adding smaller volumes of organic monomer.[4]

Shell Wall Thickness

Because the formation of urea-formaldehyde aggregates is directly responsible for the outer shell wall thickness, the same parameters that control surface morphology will control the thickness. However, the inner shell wall, which is composed of a thin layer of EMA copolymer surrounded by cross-linked layers of poly(urea-formaldehyde), forms early in the reaction and its characteristics are independent of subsequent reaction variables.[4] This may be due to stoichiometric limitations of the reagents. The poly(urea-formaldehyde) may interact with the EMA micelle via hydrogen bonding, and the number of these interactions is limited by available atoms at the interface.

Characterization by Infrared Spectroscopy

Previous work by White, et. al. employed the use of infrared spectroscopy to characterize the effectiveness of their self-healing system. Using the appearance of a *trans*-double bond appearing at 965 cm^{-1} as evidence of DCPD polymerization (Figure 4), the crack plane within the epoxy resin was imaged and the infrared spectrum was collected on site.[1]

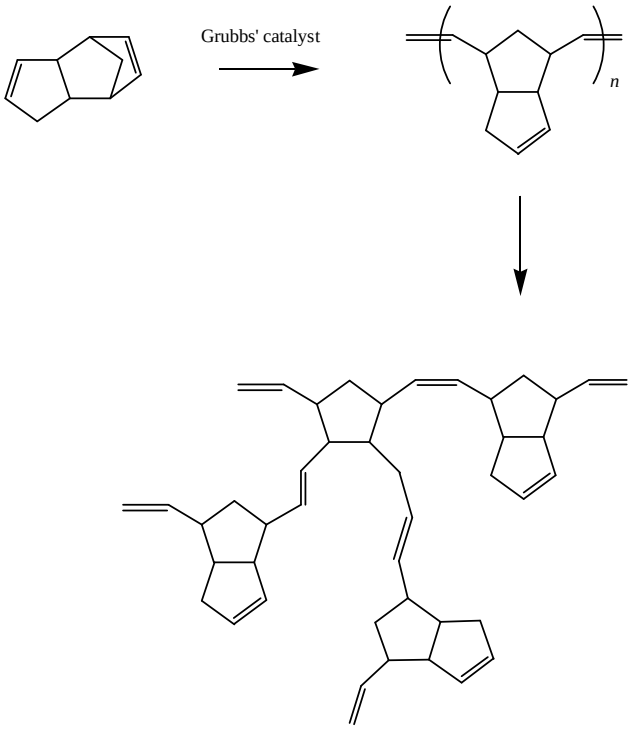

Figure 4. Ring-opening metathesis polymerization of DCPD.

The assembly of a thin film in the crack coupled with the appearance of the *trans*-double bond stretch at 965 cm^{-1} proved that the material had in fact "self-healed." Gathering spectral evidence at the site of damage in a material is not an easy task. White, et. al. obtained infrared spectra from a damaged *surface*. Scanning electron micrograph (SEM) images of the crack plane provided evidence for the thin polymeric film, which could then be analyzed. However, much of the microscale damage that occurs in materials is the

result of hidden *internal* cracks that cannot be imaged by microscopy. This makes analysis of the damage and proof of self-healing capabilities extremely difficult. Under the modified design of our self-healing system, several spectroscopic methods were explored to evidence the polymerization of the monomer within the material.

The first effort mimicked the work of White, et. al., providing infrared spectral signatures for dicyclopentadiene and its polymerized product. The subsequent spectral signatures were obtained for *microencapsulated* DCPD with and without the presence of Grubbs' catalyst. However, infrared spectral evidence for the presence of monomer or polymer could not be obtained when the microcapsules were buried in the material matrix. Shown in Figure 5 is the infrared spectrum of liquid-phase dicyclopentadiene. The intense, sharp peaks at 755 cm^{-1} and 727 cm^{-1} represent the *cis*-RCH=CHR bending modes.

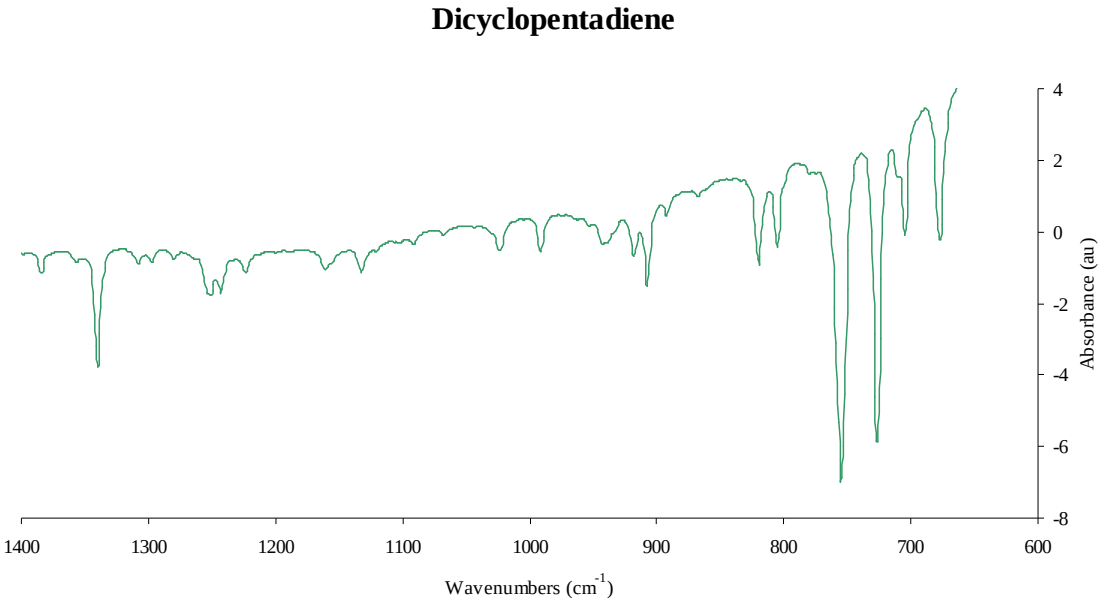

Figure 5. FTIR spectrum of liquid DCPD.

Shown in Figure 6 is DCPD in the presence of second generation Grubbs' catalyst. The diminishing of the peaks at 755 cm^{-1} and and 727 cm^{-1} as well as the growth of a new peak at 976 cm^{-1} are evidence for the polymerization of DCPD.[7] The new peak is representative of the C-H bending mode of a *trans*-double bond. These changes are highlighted in Figure 7.

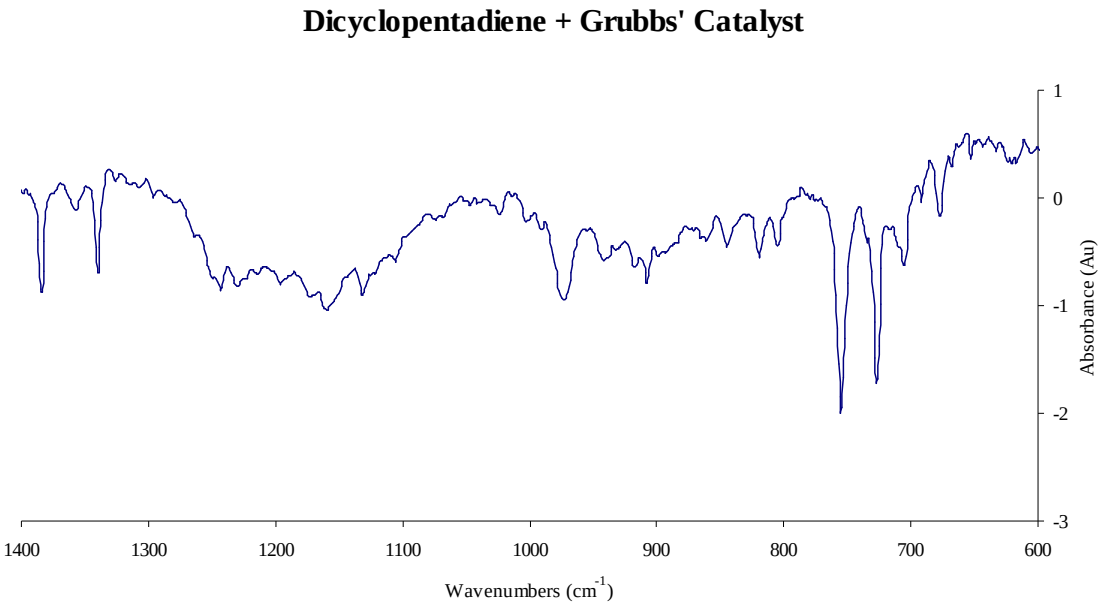

Figure 6. FTIR spectrum of DCPD in the presence of Grubbs' catalyst.

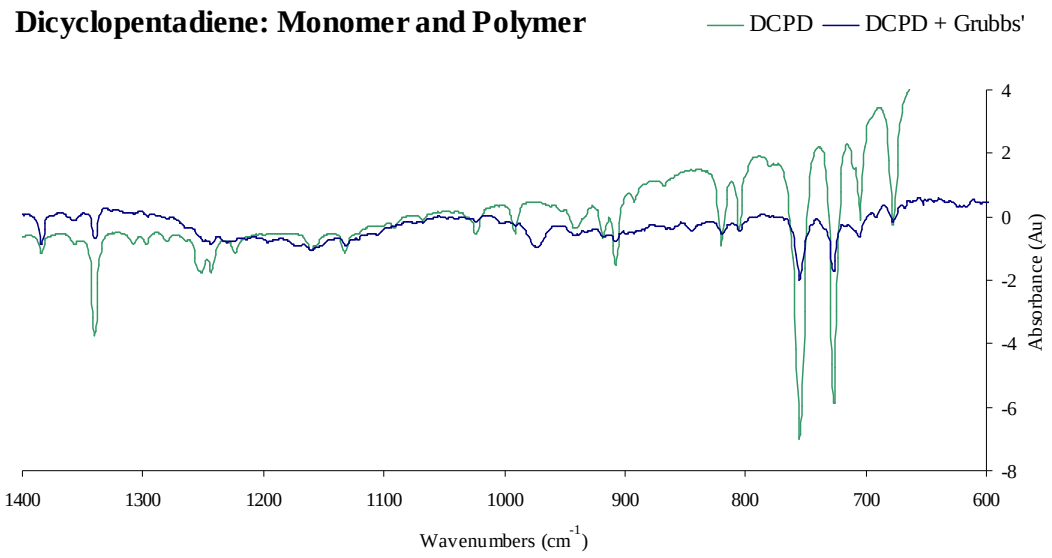

Figure 7. Comparison of FTIR spectra of DCPD with and without the presence of Grubbs' catalyst.

While the infrared spectrum for microencapsulated DCPD (Figure 8) clearly shows the absence of the *trans*-double bond peak at 976 cm^{-1}, the expected *cis*-double bond peaks at 755 cm^{-1} and 727 cm^{-1} are also absent. The only evidence for the presence of dicyclopentadiene within the microcapsule is the sharp peak at 668 cm^{-1} corresponding to the $-CH_2$ bending mode. This peak is too prominent to represent the $–CH_2$ associated with poly(urea-formaldehyde). [5b]

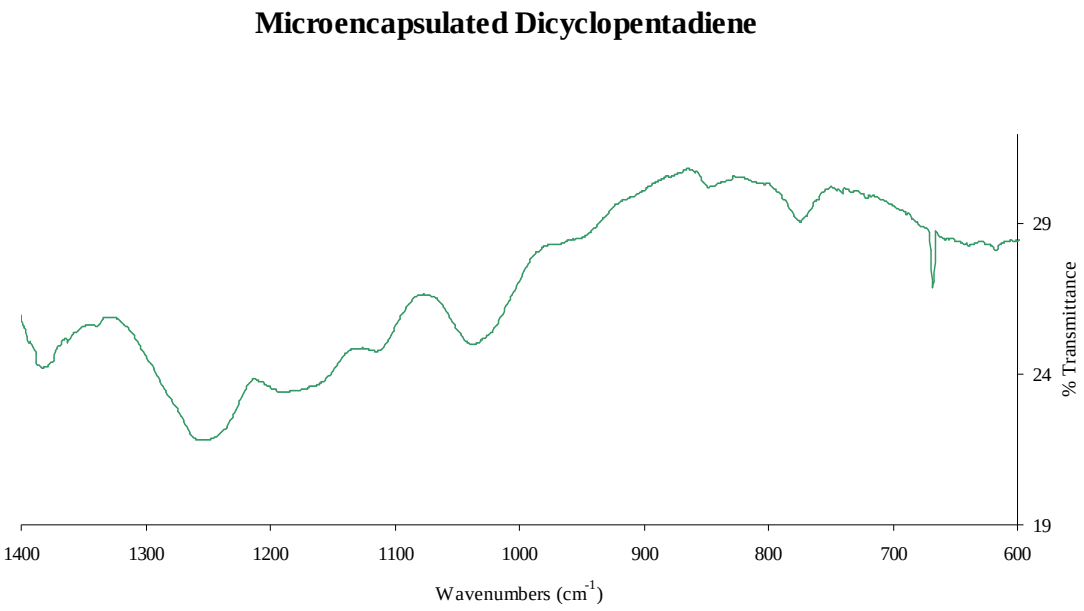

Figure 8. FTIR spectrum of microencapsulated DCPD.

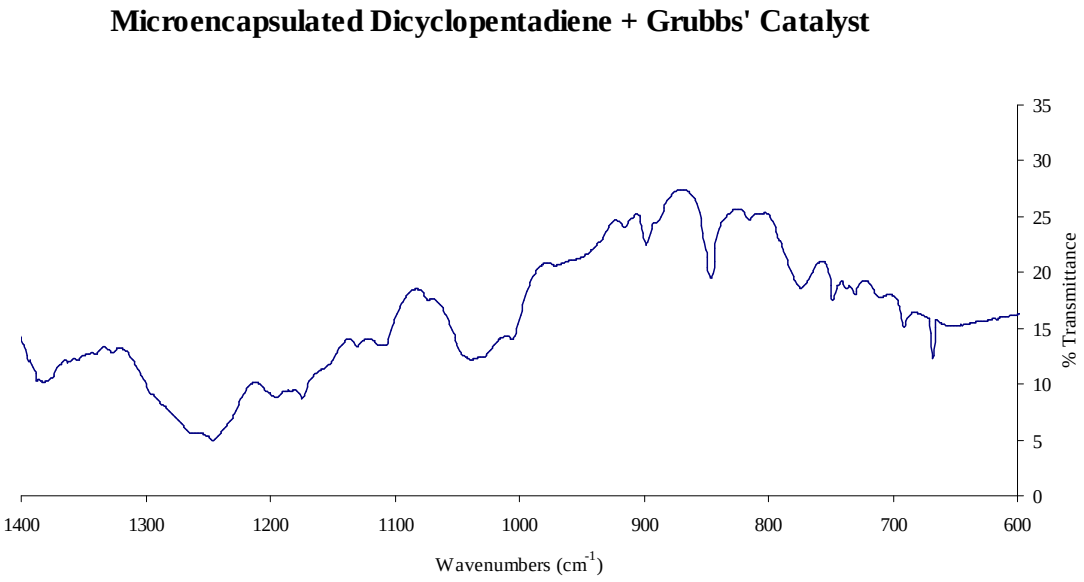

Figure 9. FTIR spectrum of microencapsulated DCPD in the presence of Grubbs' catalyst.

Figure 9 shows the appearance of a peak at 976 cm^{-1}, though very weak and much broader than expected. Figure 10 highlights the differences between the spectra of DCPD microcapsules with and without Grubbs' catalyst.

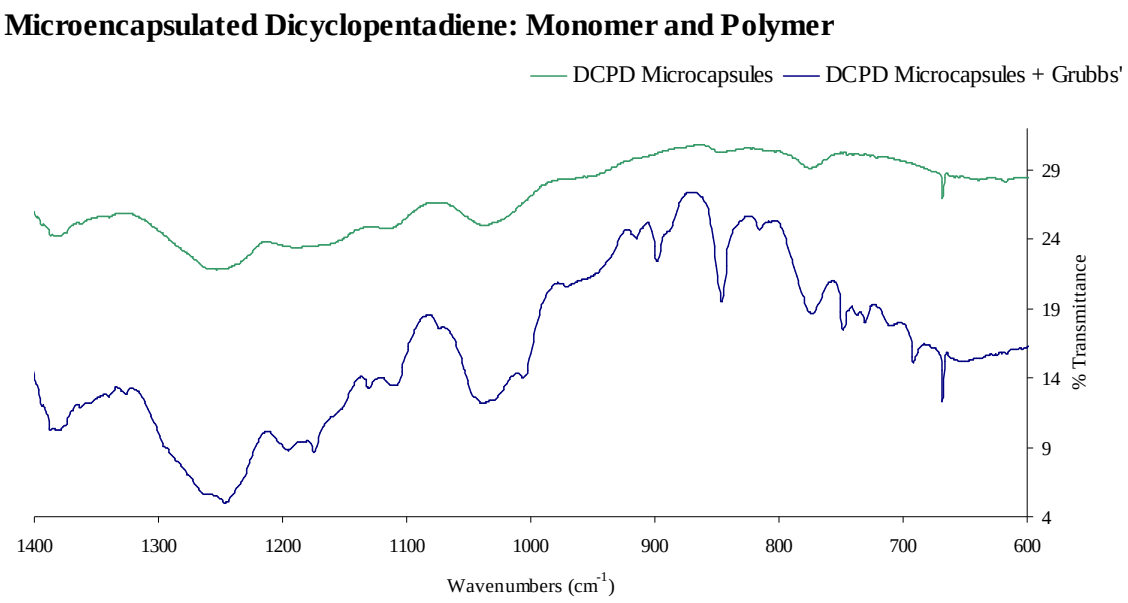

Figure 10. Comparison of FTIR spectra of DCPD microcapsules with and without the presence of Grubbs' catalyst.

To be sure that the presumed *trans*-double bond peak present in Figure 10 represents polymerized DCPD, Figure 11 shows the IR spectrum of Grubbs' second generation catalyst. There is no peak present between 1010 cm^{-1} and 929 cm^{-1}.

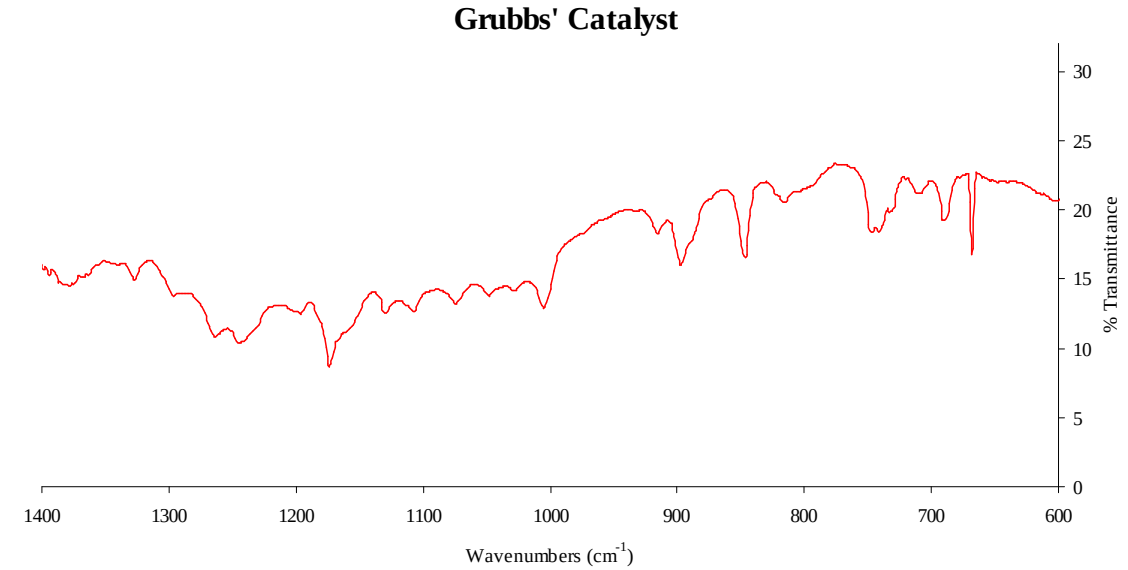

Figure 11. FTIR spectrum of Grubbs' catalyst.

Analogous methods to those used to determine the polymerization of DCPD can be used to determine the polymerization of cyclooctadiene. This monomer readily undergoes ROMP in the presence of second generation Grubbs' catalyst (Figure 12), and the polymerized product contains long chains with primarily *trans*-double bonds.[8]

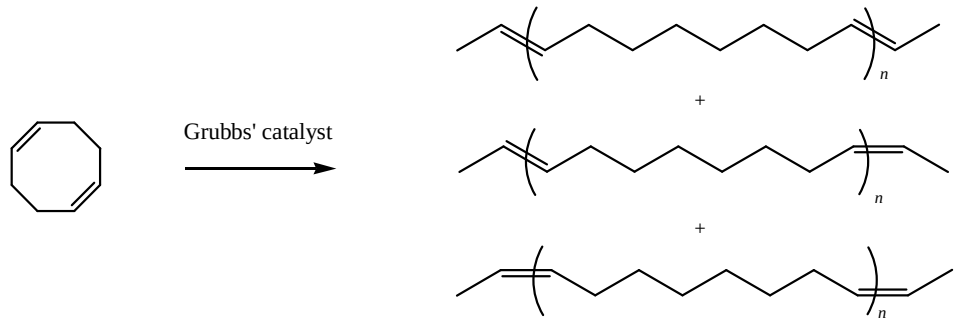

Figure 12. ROMP products of COD in the presence of second generation Grubbs' catalyst; note that many of these bonds undergo spontaneous *cis-trans* isomerization following the polymerization, resulting in primarily *trans*- polymeric chains.

Figure 13 shows the IR spectrum of liquid COD. The sharp, prominent peaks at 800 cm^{-1}, 723 cm^{-1}, 709 cm^{-1} and 652 cm^{-1} correspond to *cis*-RCH=CHR bending modes. Their broadening into a single peak at 739 cm^{-1} upon interaction with Grubbs' catalyst is clear in Figure 14, as is the appearance of a *trans*-double bond peak at 970 cm^{-1}.

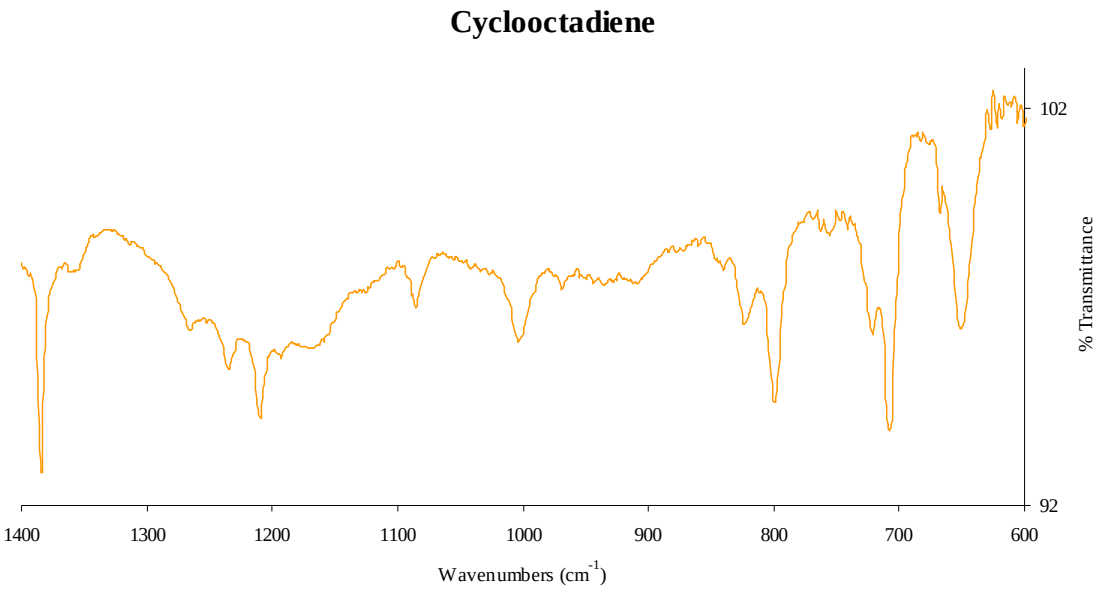

Figure 13. FTIR spectrum of liquid cyclooctadiene.

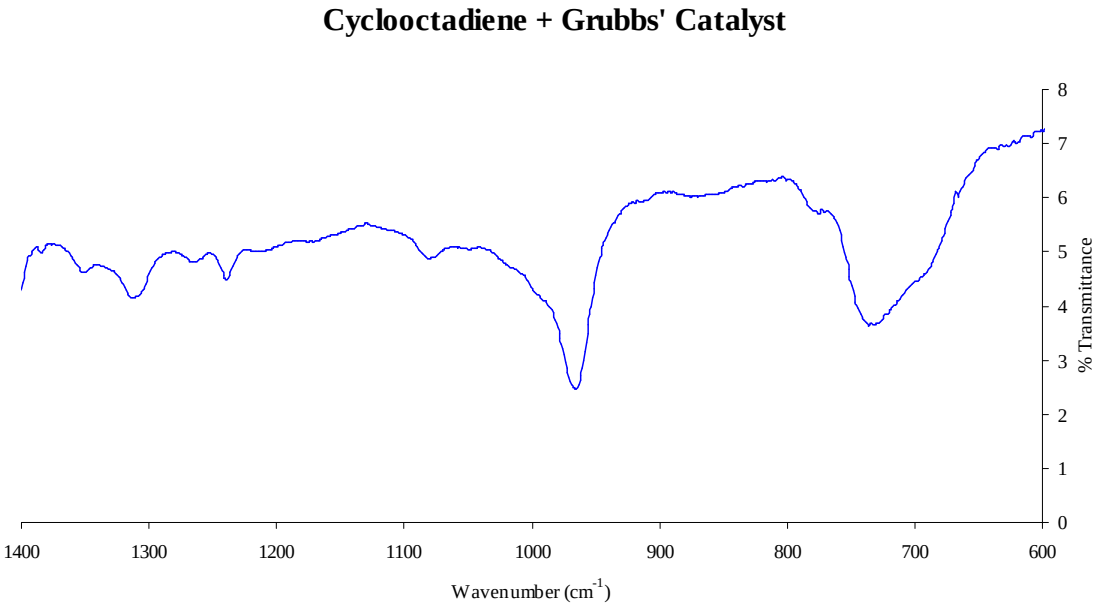

Figure 14. FTIR spectrum of cyclooctadiene in the presence of Grubbs' catalyst.

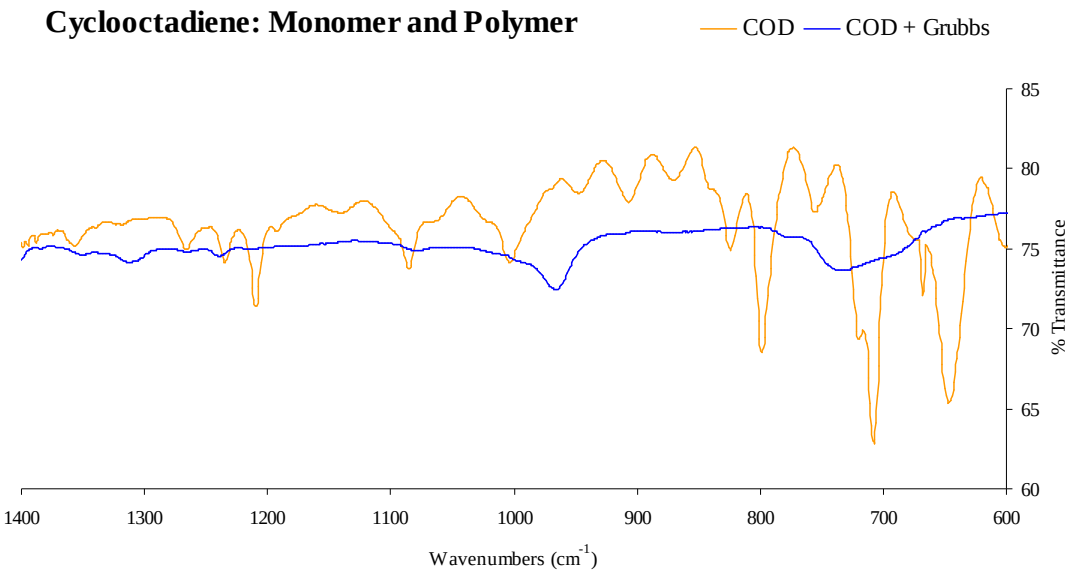

Figure 15. Comparison of FTIR spectra of COD with and without the presence of Grubbs' catalyst; note that the y values of the COD + Grubbs' spectrum were systematically increased by 70 units to highlight the appearance of the *trans*-double bond peak.

The characterization of microencapsulated cyclooctadiene and its polymerization proved quite successful. Even in the presence of strong C-O and C-N stretches from the poly(urea-formaldehyde), the appearance of the *trans*-double bond peak at 970 cm^{-1} is very apparent (Figures 16-18).

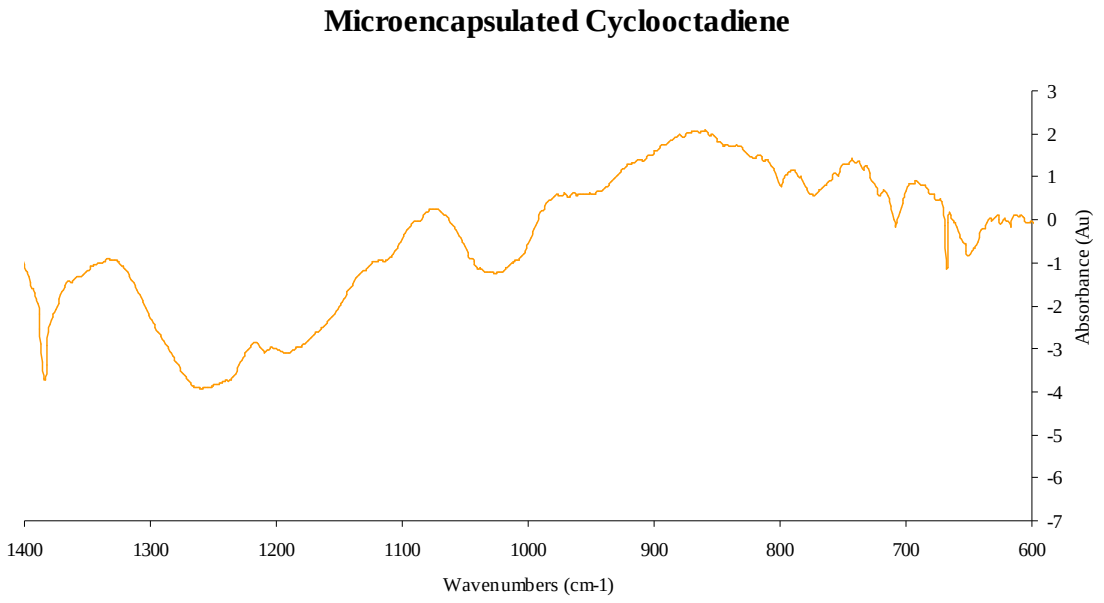

Figure 16. FTIR spectrum of microencapsulated COD.

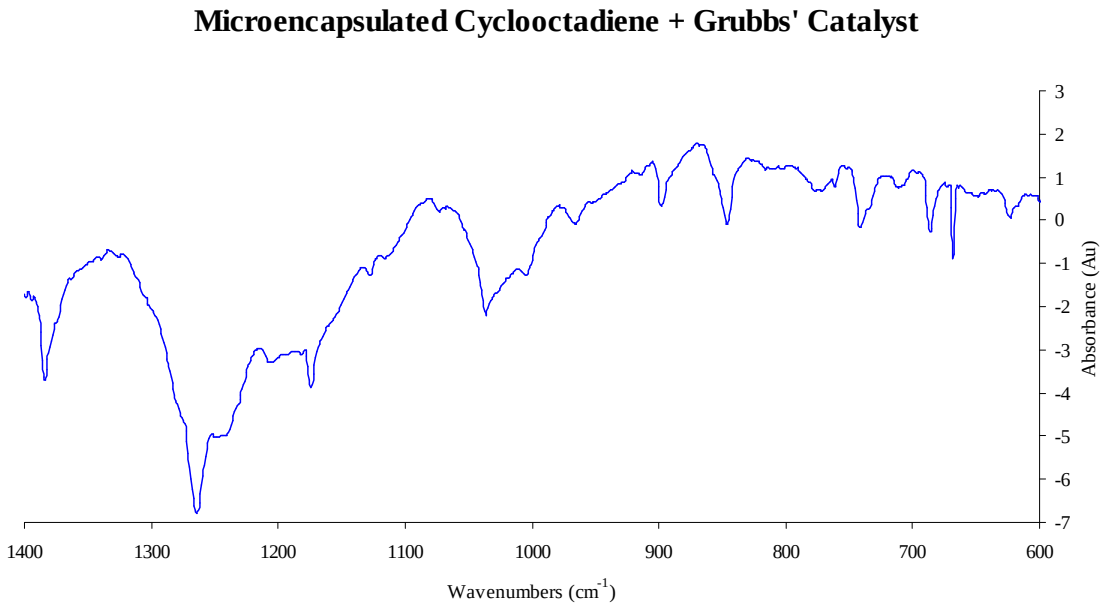

Figure 17. FTIR spectrum of microencapsulated COD in the presence of Grubbs' catalyst.

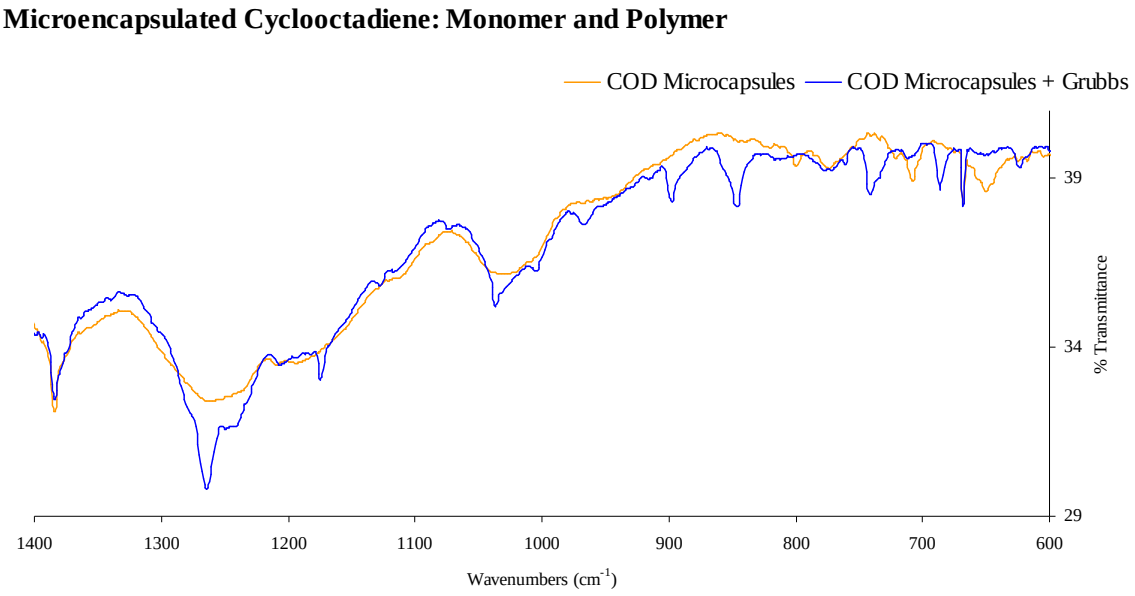

Figure 18. Comparison of microencapsulated COD with and without the presence of Grubbs' catalyst.

Unsuccessful attempts were made to achieve infrared spectral evidence of DCPD and COD polymerization from within PS, SIS, and PMMA polymeric matrices of the self-healing materials. These investigations are still active, but are hindered by heavy absorption bands from these polymers in the "fingerprint" region of the infrared spectra.

The data obtained from infrared spectroscopy not only reveals the presence of microencapsulated DCPD and COD, but can be used to distinguish each monomer from its polymerized product. While this method is useful for the characterization of microcapsules and their contents, it proves futile once the microcapsules are embedded in low concentrations into a polymer network.

Characterization by Fluorescence

One useful property of the microcapsule shell is its intense fluorescence. The confocal image of the self-healing system (Figure 19) reveals the strong emission of the microcapsules upon excitation with 543 nm light. The red fluorescence is very likely due to excitation of the microcapsule shell (poly(urea-formaldehyde)). This explains its presence on the outer circumference of the microcapsules and fragments in the polymer matrix.

The apparent green "fluorescence" found almost exclusively within the microcapsule is actually the reflection of the green laser from microencapsulated DCPD. The appropriate wavelength required to selectively excite DCPD was not available in the instrument from which the image in Figure 19 was obtained. The FV1000 is designed for biological species, so the available lasers are limited to lower-energy wavelengths. However, selective excitation of DCPD could be obtained using a simple fluorometer.

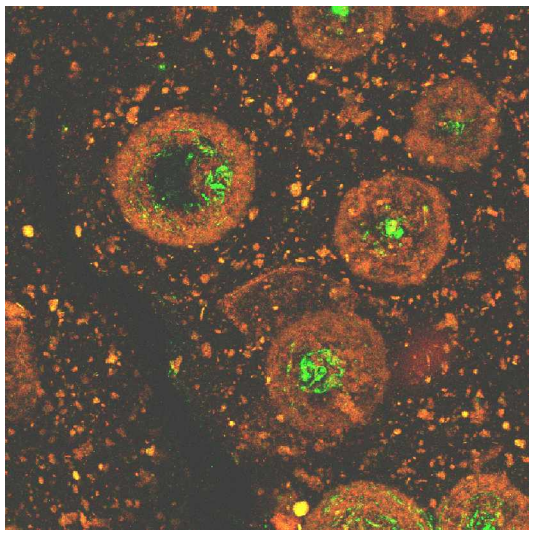

Figure 19. Confocal laser microscope image of poly(urea-formaldehyde) microcapsules filled with DCPD in polystyrene-polyisoprene-polystyrene block copolymer; image collected from the Olympus FV1000.

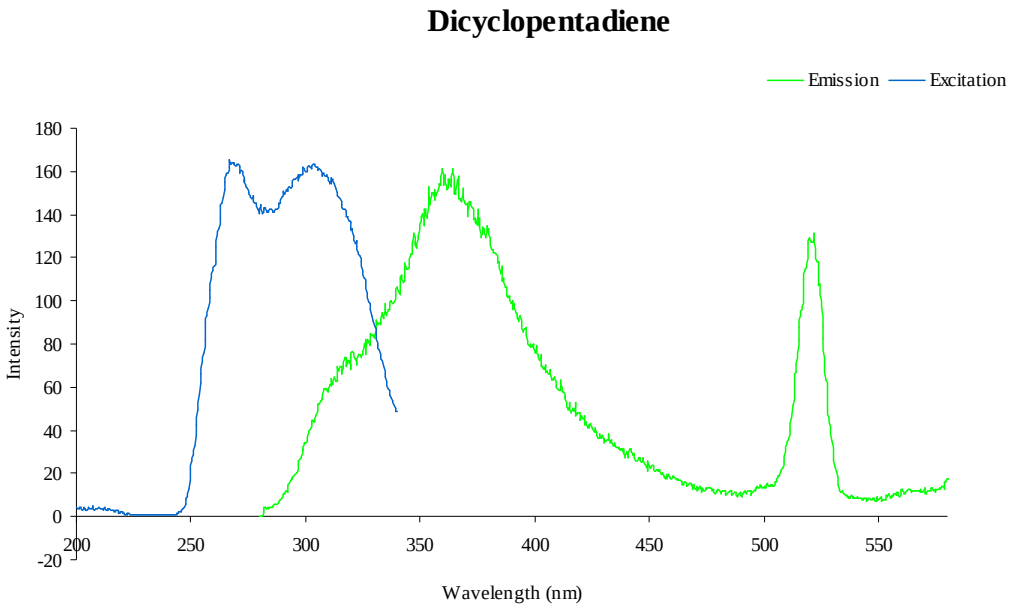

Figure 20. Emission and excitation spectra of liquid DCPD; λ_{ex} = 268 nm.

Excitation of liquid DCPD produced emission maxima at 360 nm and 522 nm (Figure 20). These emission peaks were monitored during the excitation of microcapsules in order to selectively excite the monomer from within the shell.

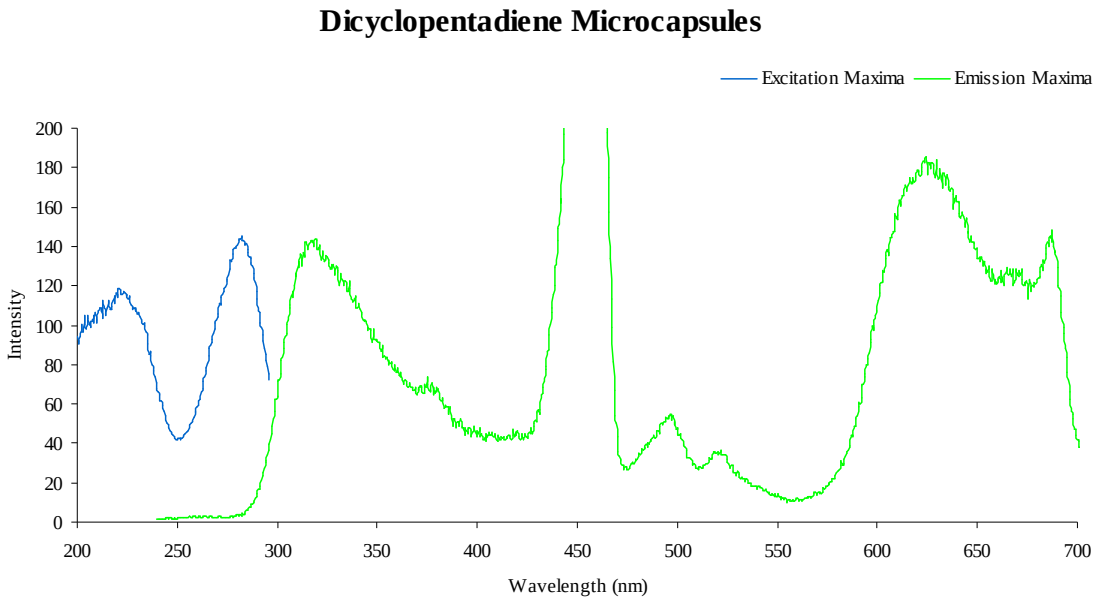

Figure 20. Emission and excitation spectra of microcencapsulated DCPD; λ_{ex} = 220 nm; note that the intense peak at 450 nm is the result of an instrumental artifact.

The peak at 522 nm is weak, but evident, in the emission spectrum for microencapsulated DCPD (Figure 21). However, the peak at 360 nm is buried under more intense emission peaks from the microcapsule shell. The large emission at 628 nm supports the assignment of red fluorescence in the confocal image to the poly(urea-formaldehyde) shell.

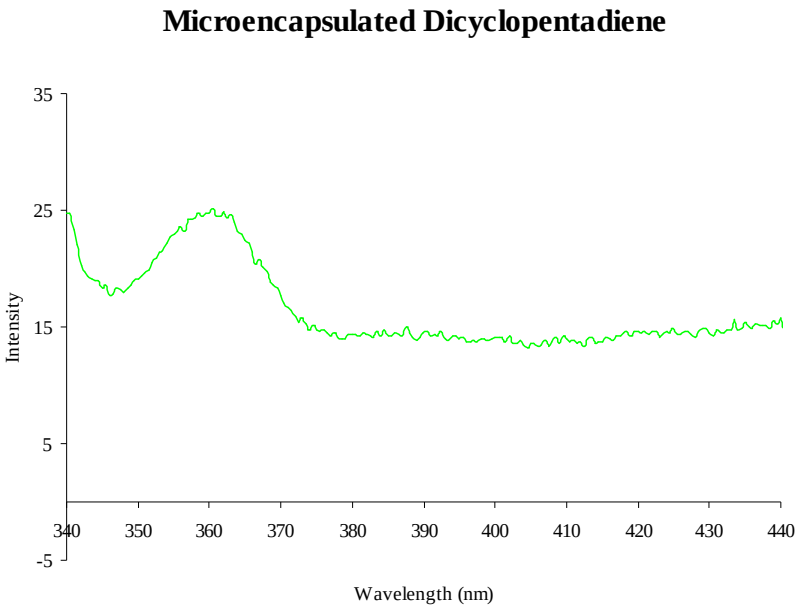

Figure 22. Emission spectrum of microencapsulated DCPD; λ_{ex} = 320 nm.

Shown in Figure 22 is the selective excitation of microencapsulated DCPD, which can be exploited in combination with confocal imaging in the future. A material into which microencapsulated DCPD is embedded can be imaged by a confocal lens and excited with 320 nm light in order to illuminate the monomer within the microcapsule. Any cracks into which the monomer has leaked will be illuminated as well, providing a profile of the damage within the material. The microcapsulated COD has not yet shown selective fluorescence, but this goal is currently being pursued.

Fluorescence microscopy proves to be a powerful tool for imaging microcapsules in a polymeric matrix. Coupling the use of a confocal lens with selective excitation of each component in the image plane may prove valuable for analysis of the damage that exists beneath the surface.

Characterization by Raman Spectroscopy

Poly(DCPD) can be distinguished from DCPD using Raman spectroscopy. By monitoring the emergence of a peak at 1660 cm^{-1}over time, the extent of DCPD polymerization can be determined.[9] While other spectral distinctions can be made between monomer and polymer, these changes are subtle.

Shown in Figure 23 is the Raman spectrum of microencapsulated DCPD, obtained by focusing the laser inside the microcapsule. The peaks in this spectrum differ systematically from the literature by 100 cm^{-1}. Although the reason for this bathochromic shift has not been determined, all attempts to confirm the presence of poly(DCPD) will be based upon the emergence of a peak at 1560 cm^{-1}.

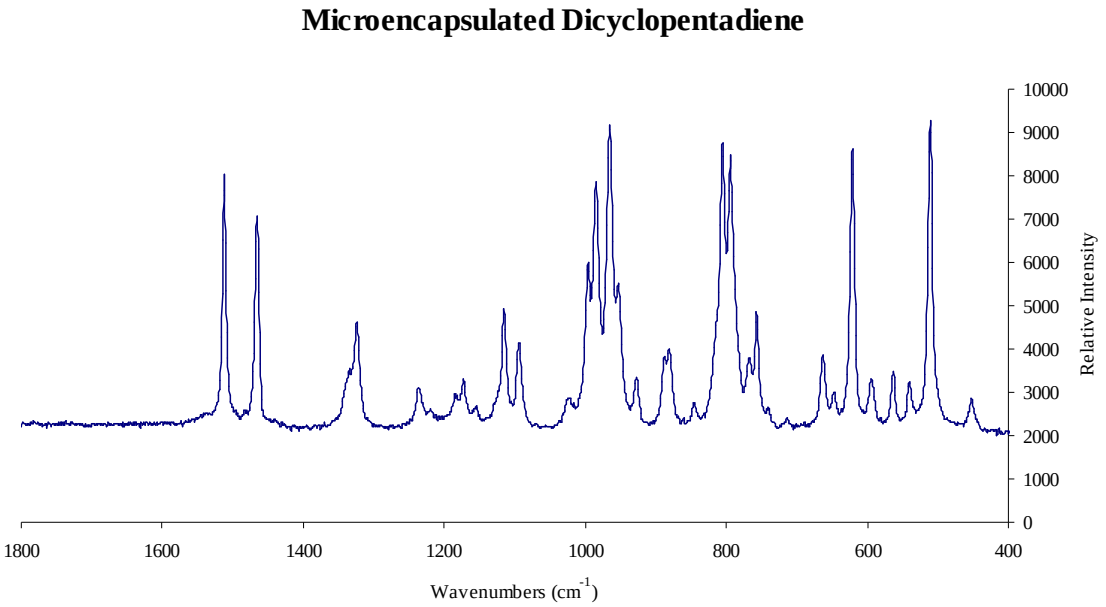

Figure 23. Raman spectrum of microencapsulated DCPD.

Unlike the infrared spectrum, the Raman spectrum obtained from microencapsulated DCPD (Figure 23) is almost identical to that of its liberated form. The coupling of the Raman laser to a microscope minimizes any scattering from the microcapsule shell. However, monitoring the polymerization of DCPD proved to be more difficult. The sample preparation (gentle crushing of the microcapsules with catalyst) necessitates the presence of microcapsule shell and Grubbs' catalyst in the liberated DCPD. Determining the optimum focus for the laser requires *finding* the polymer in the midst of the other components. Though repeated attempts were made to achieve this optimum focus, the resulting Raman spectra were inconclusive.

Microencapsulated DCPD is barely detectable from within the poly(SIS) matrix. Shown in Figure 24 and 25 are the Raman spectra of poly(SIS) and a DCPD microcapsule within poly(SIS) matrix. The spectrum in Figure 25 contains peaks at 1514 cm^{-1} and 1467 cm^{-1}, corresponding to DCPD. This is promising evidence for the detection of the monomer in a self-healing system. However, the large peak at 1567 cm^{-1} from poly(SIS) prohibits the detection of poly(DCPD) within the matrix. Figure 26 highlights the differences between the spectra in the region between 1450 cm^{-1} and 1550 cm^{-1}.

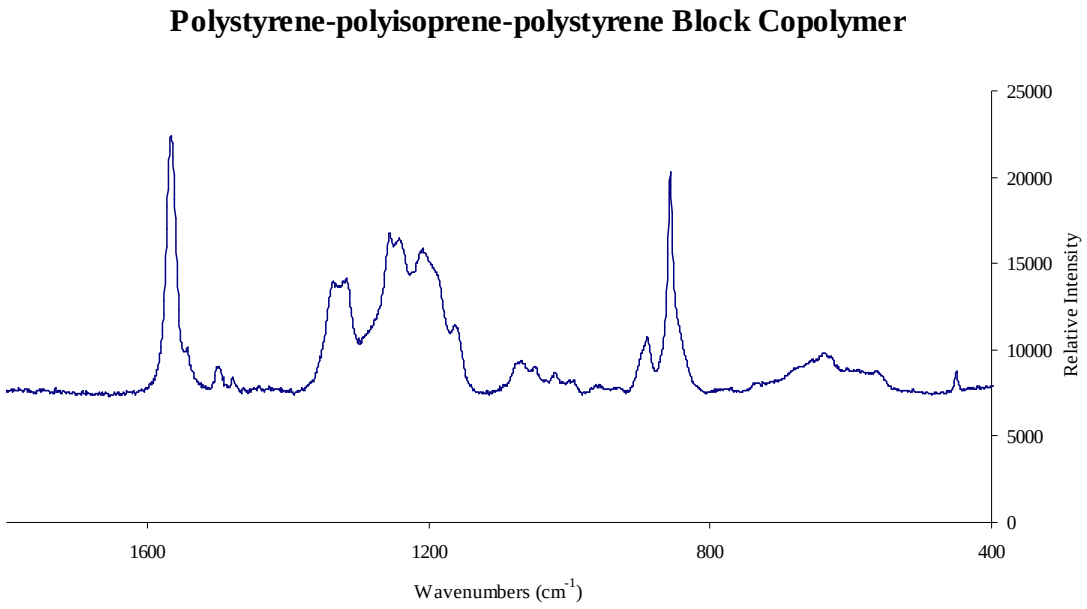

Figure 24. Raman spectrum of poly(SIS).

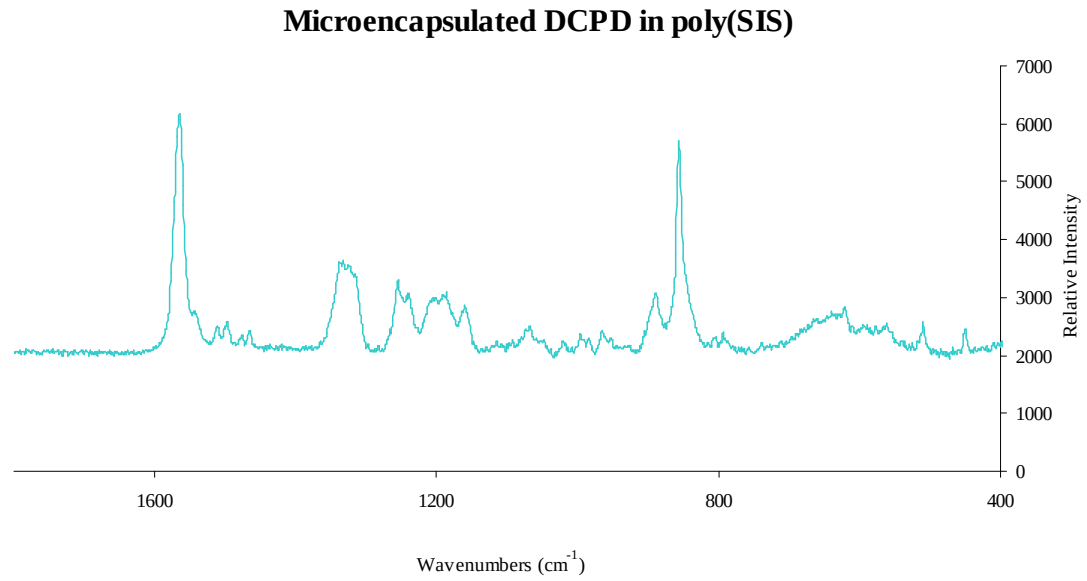

Figure 25. Raman spectrum of microencapsulated DCPD within poly(SIS) matrix.

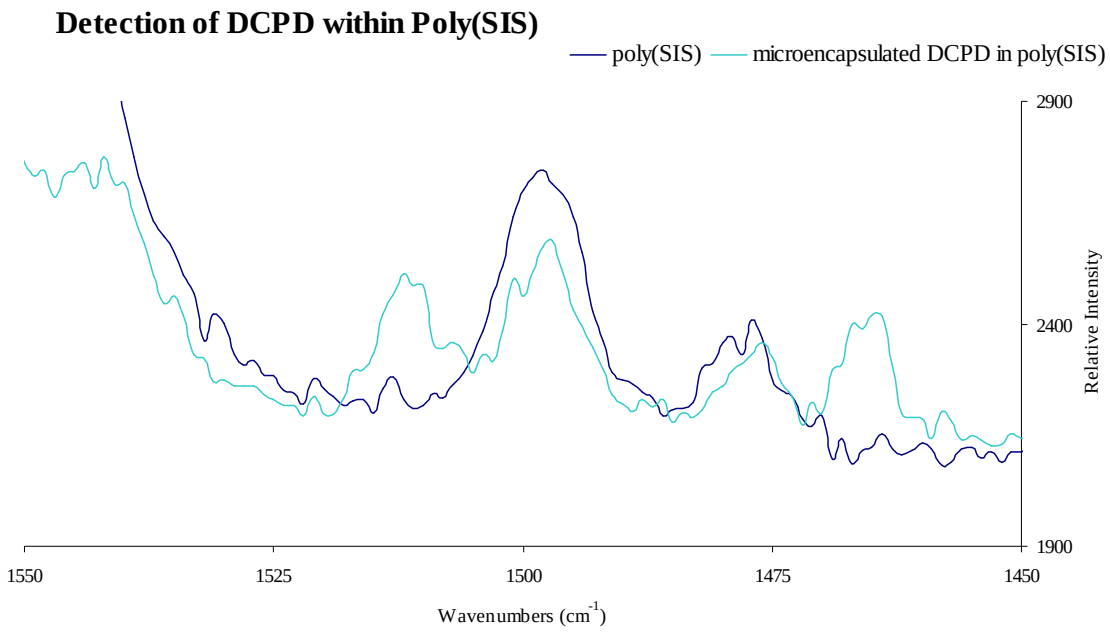

Figure 26. Highlighting the detection of microencapsulated DCPD within poly(SIS) matrix by the appearance of peaks at 1514 cm^{-1} and 1467 cm^{-1}.

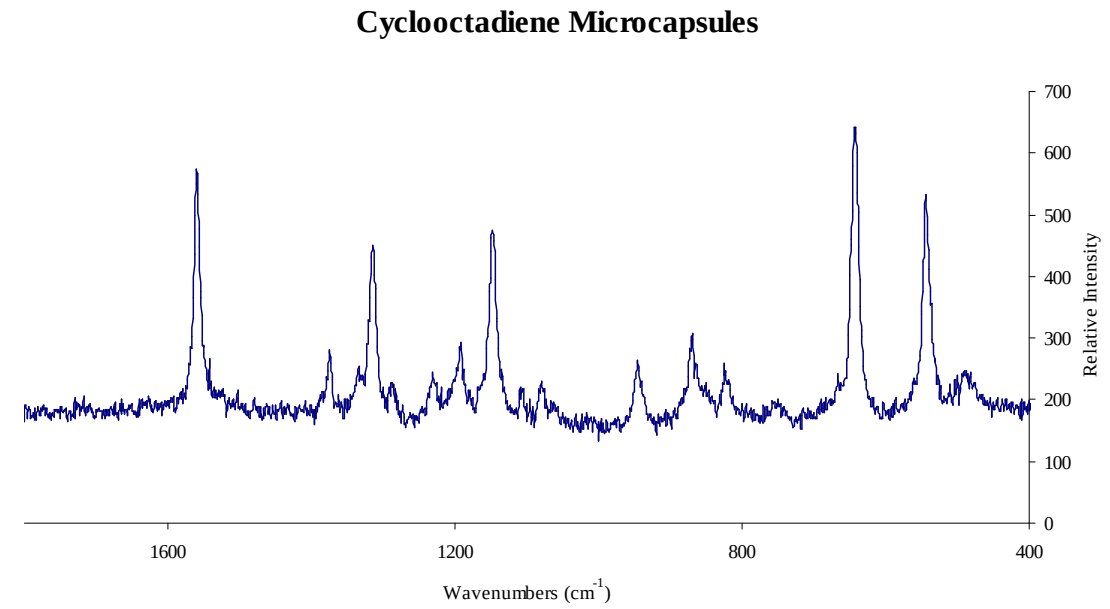

Figure 27. Raman spectrum of microencapsulated COD.

The Raman spectrum for COD within the microcapsule resembles the spectrum predicted in the literature for free COD.[10] The same bathochromic shift of 100 cm^{-1} of

microencapsulated monomer to liberated monomer was found for COD that was found DCPD.

The preliminary results for the detection of microencapsulated cyclooctadiene are encouraging (Figure 27). However, no studies have been conducted to monitor the polymerization of COD by Raman spectroscopy. Hence, attempts to characterize poly(COD) by Raman are currently under investigation. Furthermore, attempts to detect COD within a polymer matrix have been unsuccessful.

Characterization by Scanning Electron Micrograph

While literature containing similar syntheses[4-6] was used as a prediction of the characteristics of our microcapsules, analysis of SEM images confirmed these predictions. Figures 28-33 show images containing representative samples from both DCPD and COD microcapsules.

The image of a cracked microcapsule in Figure 28 shows clearly the rough surface topology of the outer shell. The microcapsule in Figure 29 has been pulled apart to reveal the smooth inner membrane. The image in Figure 30, along with similar images that contain a representative group of microcapsules, was used to estimate the average diameter of a DCPD microcapsule to be about 160 microns.

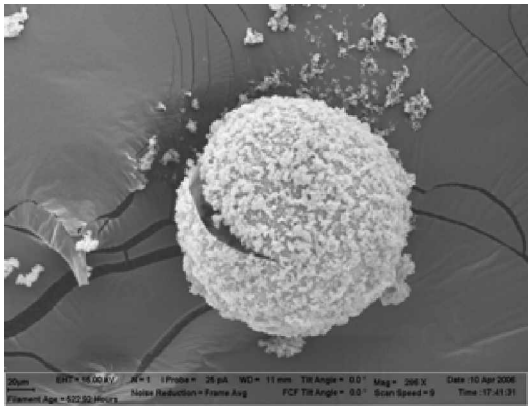

Figure 28. SEM image of a DCPD microcapsule.

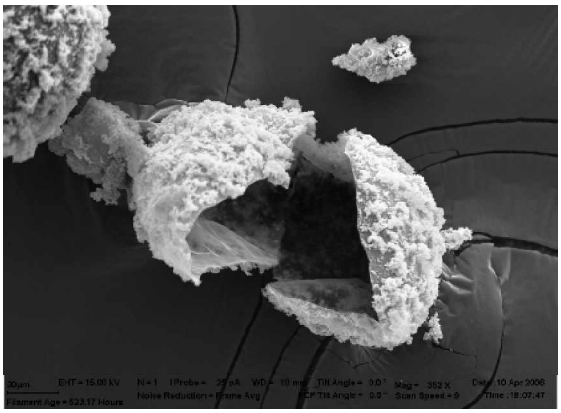

Figure 29. SEM image of a DCPD microcapsule.

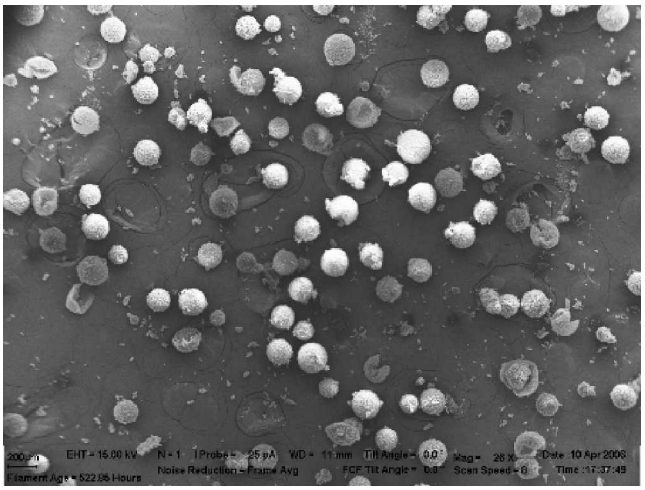

Figure 30. SEM image of DCPD microcapsules.

The COD microcapsules, as revealed by the images in Figures 31-33, consisted of a slightly smoother outer surface morphology and more free aggregated poly(urea-formaldehyde). The average microcapsule diameter was estimated to be about 50 microns. Modifications to the synthesis of COD microcapsules are currently being developed and applied to increase the diameter and the roughness of the outer shell. Some of these modifications include a reduced agitation rate and a decreased volume of COD. Preliminary results suggest that these modifications are successful, but optimum conditions for the synthesis of microencapsulated COD have yet to be determined.

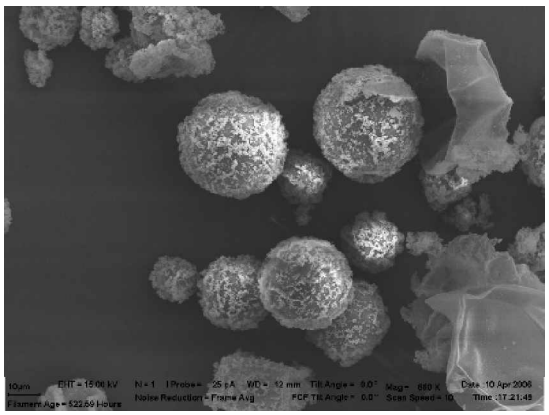

Figure 31. SEM image of COD microcapsules.

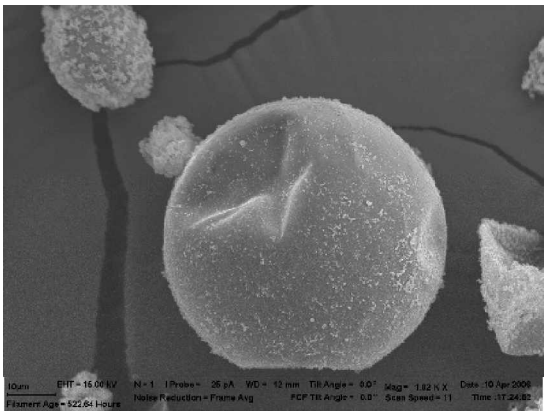

Figure 32. SEM image of COD microcapsule

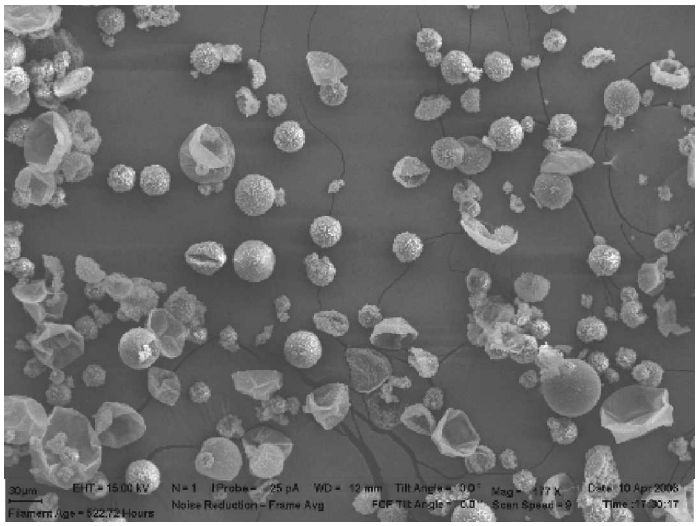

Figure 33. SEM image of COD microcapsules

Experimental

Synthesis of Dicyclopentadiene Microcapsules

In a 1000-mL beaker, 200 mL H_2O and 50 mL 2.5 % wt. EMA copolymer were combined under 350 rpm agitation, followed by the addition of 5.00 g urea, 0.50 g resorcinol, and 0.50 g ammonium chloride. Several drops of 10% wt. NaOH were added to raise the pH to 3.50 and 3 drops of 1-octanol were added to eliminate surface bubbles. Sixty mL of liquid DCPD were added and the reaction mixture was allowed to stabilize. After 10

minutes, 12.67 g of 37% aqueous formaldehyde were added. The reaction was heated at a rate of about 1°C per minute until it reached 55°C. The agitation rate was increased to 550 rpm and continued under agitation for 6 hours. After cooling, the microcapsules were separated from the aqueous phase by suction filtration.

Synthesis of Cyclooctadiene Microcapsules

An analogous procedure to that of DCPD microcapsule synthesis was used to synthesize COD microcapsules, with the following variations:

- The initial stirring rate was 750 rpm, which was decreased to 550 rpm upon heating.
- Eighty mL of COD were added to the reaction mixture
- Agitation continued after heating for 4 hours.

Preparation of Modified Self-Healing Design

Twenty grams of poly(SIS) were dissolved in 50 mL toluene under agitation to achieve a homogeneous mixture. Then, 2.0 g microcapsules were dispersed in the mixture followed by 0.001 g second generation Grubbs' catalyst. The mixture was poured onto silica-coated glass microscope slides.

Sample Preparation and Instrument Specifications

All infrared spectra were collected from KBr samples and recorded on a Nicolet 510P FTIR spectrometer. The fluorescent confocal image was collected from an Olympus FV1000 under operation of a Helium-Neon 543 nm laser. Emission and excitation

maxima were collected from a Perkin-Elmer LS50B fluorometer. All Raman spectra were collected with a Renishaw 1000B micro-Raman spectrometer under the operation of a 785 nm SDL diode laser. SEM images were collected on gold-sputtered samples from LEO 1430 scanning electron micrograph.

Future Work

Having obtained partial FTIR, Raman, and fluorescence spectral profiles of microencapsulated monomers DCPD and COD and poly(DCPD), I will focus my initial effort on improving the detection of microencapsulated monomer within a poly(SIS) matrix. In addition, methods to distinguish polymer from monomer within the self-healing material are currently being explored. Once effective distinction of monomer and polymer is achieved using the spectroscopic methods described in this paper, the capabilities of our modified self-healing design can be better evaluated. Spectroscopic evaluation of damage in conjunction with mechanical testing will aid in the design of a material with enhanced mechanical properties.

Acknowledgements

I would like to express my sincere gratitude to my peers and co-workers for offering their knowledge and support so freely, and to Jeff Zaleski and Mircea Chipara for allowing me the opportunity to do research under their guidance.

References

1. White, S.R., Sottos, N.R., Geubelle, P.H., Moore, J.S., Kessler, M.R., Sriram, S.R., et al. *Nature* **2001**, *409*, 794-797.

2. a) Brown, E.N., Sottos, N.R., White, S.R. *Composites A* **2003**, *34*, 743-753.
   b) Brown, E.N., White, S.R., Sottos, N.R. *Comp. Sci. Tech.* **2005**, *65*, 2466-2473.
   c) Brown, E.N., White, S.R., Sottos, N.R. *Comp. Sci. Tech.* **2005**, *65*, 2474-2480.

3. Bresee, J.C., Flanary, J.R., Goode, J.H., Watson, C.D., Watson, J.S. *Nucleonics* **1956**, *14*, 75-81

4. Brown, E.N., Kessler, M.R., Sottos, N.R., White, S.R. *J. Microencapsulation* **2003**, *20*, 719-733.

5. a) Sliwka, Wolfgang *Angew. Chem., Int. Ed. Engl.* **1975**, *14*, 539-550
   b) Tseng, Y.H, Fang, M.H., Tsai, P.S., Yang, Y.M. *J. Microencapsulation* **2005**, *22*, 37-46

6. Alexandridou, S., Kiparissides, C., Mange, F., Foissy, A. *J. Microencapsulation* **2001**, *18*, 767-781

7. Constable, G.S., Lesser, A.J., Coughlin, B. *J. Polym. Sci. B.* **2003**, *41*, 1323-1333

8. Hillmyer, M.A., Nguyen, S.T., Grubbs, R.H. *Macromolecules* **1997**, *30*, 718-721

9. Barnes, S.E., Brown, E.C., Corrigan, N., Coates, P.D., Harkin-Jones, E., Edwards, H.G.M. *Spectrochim. Acta A* **2005**, *61*, 2946-2952

10. Z., Xuefeng, Pulay, P. *Spectrochim. Acta A* **1993**, *49*, 257-270